Nanocrystal-induced line narrowing of surface acoustic phonons in the Raman spectra of embedded Ge_xSi_{1-x} alloy nanocrystals

X. L. Wu,[1,*] S. J. Xiong,[1] Y. M. Yang,[1,2] J. F. Gong,[1] H. T. Chen,[1] J. Zhu,[1] J. C. Shen,[1] and Paul K. Chu[3]
[1]*National Laboratory of Solid State Microstructures and Department of Physics, Nanjing University, Nanjing 210093, People's Republic of China*
[2]*Department of Physics, Southeast University, Nanjing 210096, People's Republic of China*
[3]*Department of Physics and Materials Science, City University of Hong Kong, Kowloon, Hong Kong, China*
(Received 17 September 2008; published 22 October 2008)

Raman scattering was performed on Ge_xSi_{1-x} (x=0.54 or 0.28) alloy nanocrystals embedded in amorphous Si oxide. An asymmetric, depolarized, and size-dependent low-frequency Raman peak was observed and identified as the superposition of two surface acoustic vibration modes of the alloy nanocrystals. The current theoretical models can be used to explain the mode frequencies but not the dampings observed experimentally. Based on energy-dispersive x-ray microanalysis and density-functional-theory total energy optimization of structures, a modified core-shell-matrix model in which the effects of neighboring nanocrystals in the matrix are taken into account is in good agreement with experiments. This work provides good insight into the frequencies and dampings of acoustic vibrations of the nanocrystals embedded in the matrix.

DOI: 10.1103/PhysRevB.78.165319 PACS number(s): 78.30.Fs, 63.22.−m, 61.46.Hk

I. INTRODUCTION

Low-frequency Raman scattering of semiconductor nanocrystals (NCs) has been a subject of extensive experimental and theoretical studies because of the fundamental physical interest in the small size effect.[1–11] A difficult task is the assignment of the low-frequency modes because of the complexity of the environment around the NCs. For weak vibration coupling between a continuum of homogeneous elastically isotropic NCs and their matrix, Lamb's theory[5] is suitable for identifying the acoustic modes of free or embedded NCs.[6,7,9] For strong coupling, theories proposed recently point out that the vibration eigenvector should incorporate coupling to the matrix that causes thermal fluctuations in both the amplitude and phase of the lattice vibration within the NCs.[3,12] In this case, a complex-frequency (CF) model which takes into account the action of an infinite matrix may predict the dominant frequencies of the acoustic vibration modes.[8,12] However, the calculated damping [(full width at half maximum (FWHM)] is evidently larger than the experimental data, even when ignoring additional broadening caused by the NC size distribution in a realistic system.[13] A core-shell-matrix (CSM) model may help us to improve the calculation,[14] but no corresponding result has been reported and compared to the experimental data because of the complexity of microscopic details of the shell layer.

Ge_xSi_{1-x} alloy NCs (NC-Ge_xSi_{1-x}) embedded in amorphous Si dioxide (a-SiO_2) are helpful to the exploration of acoustic vibrations of NCs because the compositions of the alloy NCs can be adjusted to alter the impedance match with the matrix. Up to now, acoustic vibrations in such systems have only been studied theoretically by lattice-dynamical calculation considering a free alloy NC.[15] The results cannot adequately explain the experimental outcome because isolated NCs do not exist. Our recent work has shown that Ge_xSi_{1-x} NCs of different sizes can be embedded in a-SiO_2 by Si-Ge-SiO_2 cosputtering and postprocessing.[16] This makes it possible to examine the different theoretical models and seek a global explanation for the frequencies and dampings of acoustic vibrations of the NCs embedded in the matrix. In this paper, we first show that two groups of NC-Ge_xSi_{1-x}-embedded samples with different x both produce two polarized acoustic vibration modes in the low-frequency Raman spectra. Numerical calculations based on the CF model adequately predict the frequencies of the two acoustic phonon modes but not the observed dampings. We next invoke both energy-dispersive x-ray (EDX) microanalysis and density-functional-theory (DFT) total energy optimization for structures on the NC interfaces and determine the composition of the interface layer linking the crystalline alloy NC with the SiO_2 matrix, ruling out the possibility that the interface could be softer than either the NC or the matrix. We next present a modified CSM model by considering a coupling between the acoustic vibrations of neighboring NCs and demonstrate that the damping can effectively be reduced, consistent with our experimental results.

II. SAMPLES AND EXPERIMENTALS

SiO_2/SiO_2:Ge:Si/SiO_2 sandwich structures were prepared on Si (100) substrates using radio frequency magnetron cosputtering. The areas of the Ge and Si chips on the silica target were P_{Ge}=4% and P_{Si}=6% (or 20%). Two groups of samples were deposited and then annealed in N_2 at various temperatures (T_a) for 10 min. More details pertaining to the sample preparation procedures can be found elsewhere.[16] X-ray diffraction results confirm that the two groups of samples containing NC-$Ge_{0.54}Si_{0.46}$ and NC-$Ge_{0.28}Si_{0.72}$ have a diamond structure embedded in a-SiO_2 matrix. Their morphologies and size distributions were characterized by high-resolution transmission electron microscopy (HRTEM) (JEOL-2010, equipped with energy-dispersive detection of the x ray emitted by an area of about $\pi\times 2^2$ nm^2 of the sample). The Raman spectra with five polarization configurations were acquired on a T64000 triple Raman system at backscattering geometries using the 514.5

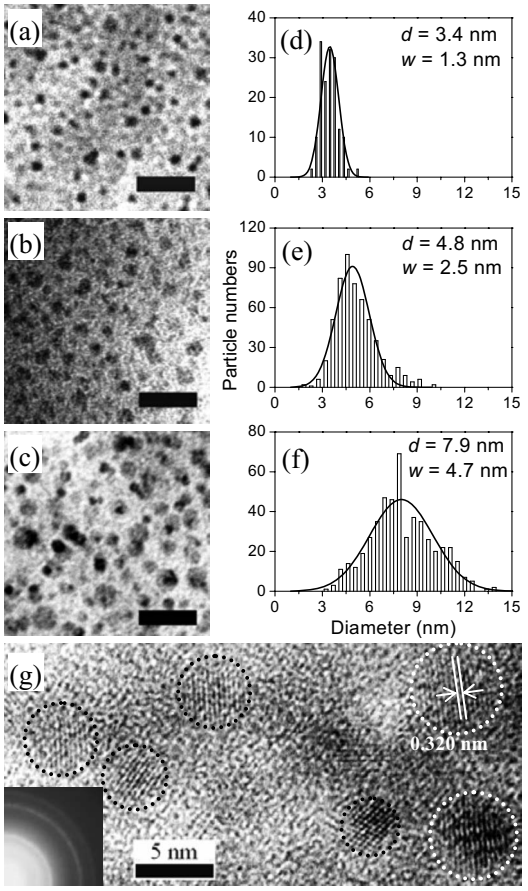

FIG. 1. [(a)–(c)] TEM images of the NC-$Ge_{0.54}Si_{0.46}$-embedded a-SiO_2 films prepared at T_a=900, 1000, and 1100 °C, respectively. The scale bars are 30 nm. [(d)–(f)] Corresponding NC size distributions with center sizes d and FWHMs w. (g) Typical HRTEM image of the sample produced at T_a=1000 °C. The inset shows the ASED pattern.

nm line of an Ar^+ laser as excitation source. All the measurements were run at room temperature.

III. RESULTS AND DISCUSSIONS

Figures 1(a)–1(c) show the transmission electron microscopy (TEM) images of the NC-$Ge_{0.54}Si_{0.46}$-embedded samples prepared at T_a=900, 1000, and 1100 °C, respectively. It can be readily observed that the NCs disperse well in a-SiO_2 films. Using Gaussian fittings, we obtain the NC size distribution and find that center size d and FWHM w increase with T_a [Figs. 1(d)–1(f)]. Figure 1(g) shows the HRTEM image of the sample prepared at T_a=1000 °C. The NCs are mostly spherical and have lattice fringes corresponding to the {111} plane of bulk SiGe alloy. The inset shows an area-selected electron diffraction (ASED) pattern and the clear diffraction rings reveal random orientations of the NCs in the film.

Figures 2(a) and 2(b) depict the depolarized and polarized Raman spectra acquired from the NC-$Ge_{0.54}Si_{0.46}$ samples. According to the three peaks around 291, 408, and 481 cm^{-1} corresponding to the well-known local optical modes (Ge-Ge, Ge-Si, and Si-Si vibrations) of GeSi alloy, the alloy NCs are shown to be NC-$Ge_{0.52}Si_{0.48}$, consistent with the x-ray diffraction results.[17] In the low frequency region, an asymmetric peak is observed. With decreasing T_a, this peak shifts toward the high-frequency side and finally merges with the TA phonon peak of the amorphous component (~77 cm^{-1}). Meanwhile, the FWHM increases and intensity decreases. The Raman shift versus the inverse of the center size is found to be linear, indicating that these low-frequency peaks arise from the surface acoustic phonon vibrations of the NC-$Ge_{0.54}Si_{0.46}$ embedded in a-SiO_2. Moreover, the Raman shift in the depolarized spectrum is smaller by several cm^{-1} than that in the polarized one.[10] The difference is larger for another group of samples containing NC-$Ge_{0.28}Si_{0.72}$, perhaps due to the different vibrational behavior of various acoustic modes.[2,13,18] To reveal the asymmetric origin of the low-frequency Raman peak, the polarization configuration dependence is determined, as was done in our previous investigation on the Ge NCs embedded in a-SiO_2.[8] Figures 3(a)–3(e) show five polarized low-frequency Raman spectra of the NC-$Ge_{0.54}Si_{0.46}$ sample prepared at T_a=1100 °C. The peak shape gradually changes with polarization configurations and it is more obvious in the spectra acquired from the NC-$Ge_{0.28}Si_{0.72}$ samples displayed in the inset. Each spectrum is composed of at least two components. Using a Lorentz function to describe the spectral broadening induced by the NC/matrix interaction and applying an inverse relationship between the energy and NC size,[19,20] spectra (a)–(e) can be divided into two peaks with the frequencies and FWHMs being ($\omega_{1\,exp}$=12.5 cm^{-1}, $\Gamma_{1\,exp}$=1.7 cm^{-1}) and ($\omega_{2\,exp}$=17.7 cm^{-1}, $\Gamma_{2\,exp}$=0.9 cm^{-1}). Here, the contribution of the NC size distribution has been deducted from the FWHM.

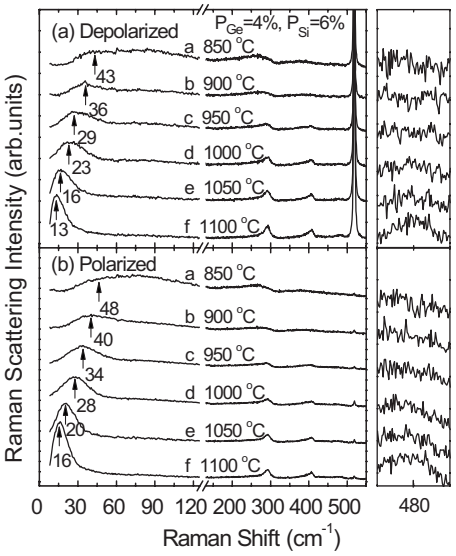

FIG. 2. Raman spectra of the NC-$Ge_{0.54}Si_{0.46}$-embedded a-SiO_2 films produced at different T_a acquired from (a) depolarized and (b) polarized configurations. The right sides of (a) and (b) show the enlarged figures in the frequency region of 450–500 cm^{-1}. In the depolarized spectrum, the strong mode at ~520 cm^{-1} is from the silicon substrate.

To theoretically identify the two components, we consider a homogeneous and isotropic nanosphere.[13,21] In the CF

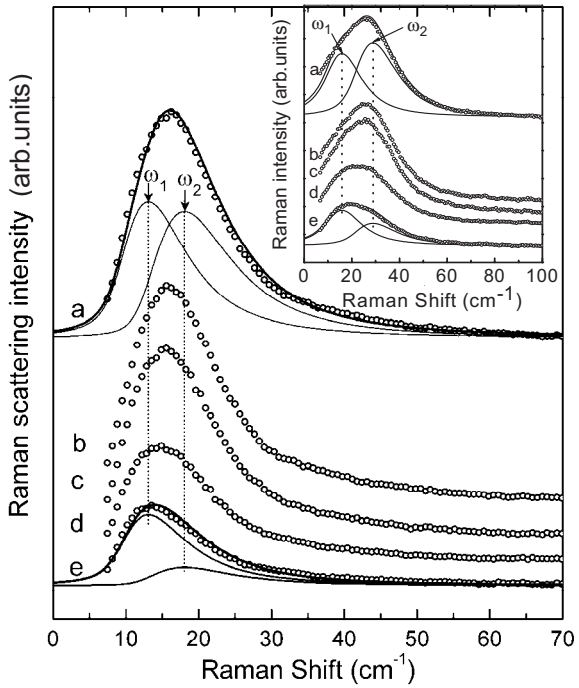

FIG. 3. Low-frequency Raman spectra of the NC-$Ge_{0.54}Si_{0.46}$-embedded a-SiO_2 film annealed at 1100 °C, acquired from five different polarization configurations [the angles between the incident and scattered light polarization directions are (a) 0, (b) 22.5, (c) 45, (d) 67.5, and (e) 90°]. The inset shows the corresponding result from another group of $Ge_{0.28}Si_{0.72}$ samples with different NC sizes.

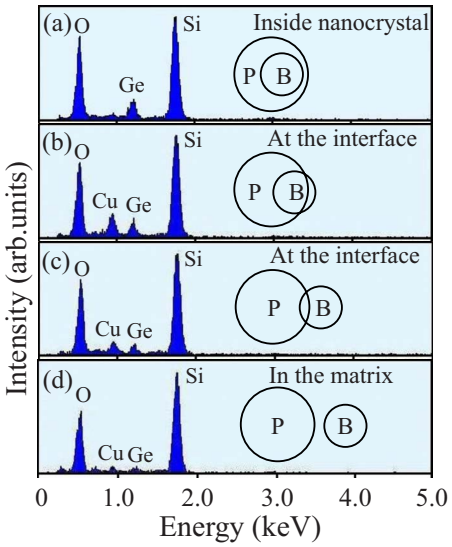

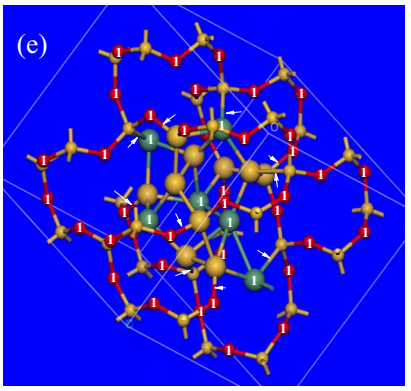

FIG. 4. (Color online) Some typical EDX spectra emitted at different positions around alloy NC: (a) inside NC, [(b) and (c)] at the interfaces, and (d) in the matrix. *P*: alloy NC; *B*: electronic beam focused at an area of about $\pi \times 2^2$ nm^2. Note that Cu signals in the spectra are from the Cu grids for the TEM measurement. (e) The optimized supercell for the GeSi NC embedded in SiO_2. Small balls in red (dark gray marked with 1) and yellow (gray) represent O and Si atoms, respectively. Big balls in yellow (gray) and gray-blue (dark gray marked with 1) represent Si and Ge atoms in the NC, respectively. The white arrows indicate the bonds at the interface between the NC and SiO_2 matrix.

model, the nanosphere is assumed to be in good contact with a macroscopic matrix. Our numerical calculations look for the complex roots $(\omega,\Gamma)_{q\,l\,n}$ of the eigenvalue equation $D=0$, where D is the determinant of a matrix not larger than (8×8).[13] The real part ω and imaginary part Γ of the complex root denote the vibration frequency and the FWHM of a Raman mode, q can be torsional (TOR) or spheroidal (SPH), l is angular momentum number, and $n \geq 0$ is the mode index. Using programs that calculate the acoustic vibrations of the NC-Si embedded in a-SiO_2,[12,13] the energy and FWHM of a spherical NC-$Ge_{0.54}Si_{0.46}$ with diameter of 7.9 nm under a core-matrix model are computed[22,23] and it is found that the best candidate for ω_1 is the TOR mode with $n=0$, $l=1$ ($\omega_{1\mathrm{cal}}=10.4$ cm^{-1}, $\Gamma_{1\mathrm{cal}}=4.7$ cm^{-1}) and for ω_2, it is the SPH mode with $n=0$, $l=2$ ($\omega_{2\mathrm{cal}}=16$ cm^{-1}, $\Gamma_{2\mathrm{cal}}=4.5$ cm^{-1}) or the TOR mode with $n=1$, $l=2$ ($\omega_{2\mathrm{cal}}=18.5$ cm^{-1}, $\Gamma_{2\mathrm{cal}}=5.2$ cm^{-1}). The calculation adequately predicts the frequencies but the FWHM values are larger than those determined experimentally.

It is believed that in the CSM model, introduction of a thin shell between the sphere and its matrix could effectively decrease the damping.[24] The key of this model is to determine the interface composition. Hence, we performed the EDX microanalyses at different positions around NCs. Figures 4(a)–4(d) show the corresponding results from some typical positions. Inside the NC, the content ratio of Ge to Si has a maximum and then gradually decreases while moving the electron beam toward the NC interface. In the matrix, the Ge content is difficult to detect. This EDX result indicates that the interface regions of the NCs have no noticeable element deficiencies. The interface layer has compositions between those of the alloy NC and the SiO_2 matrix. Here, we should mention that the oxygen content in all the EDX spectra is large, which is because each electron beam emitting the x rays penetrates through the SiO_2 surface layer of the NC. To further have insight into the structure of the interface layer, we also performed a structural optimization for GeSi NCs embedded in SiO_2 matrix based on the DFT total energy calculation. In the calculation the plane-wave basis and ultrasoft pseudopotentials with gradient exchange-correlation potential corrections are used.[25,26] The optimized supercell for the GeSi NC in SiO_2 is reported in Fig. 4(e). It can be clearly seen that the connection between the NC and SiO_2 is compact and there are no evident isolation trends between the NC and matrix.

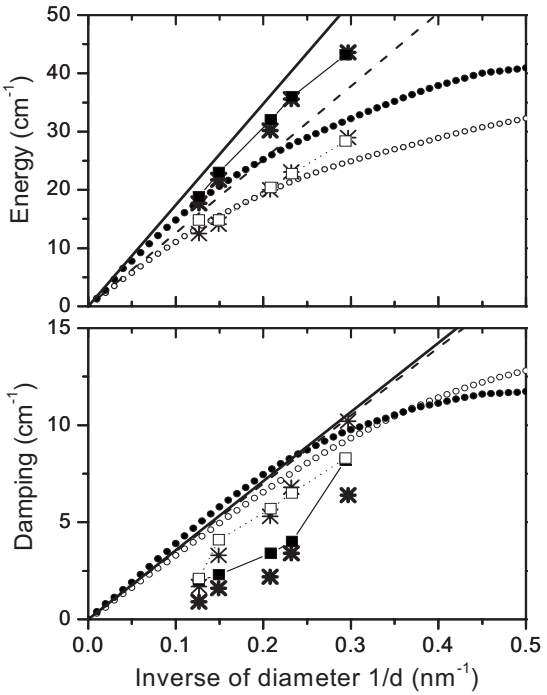

FIG. 5. Energies and dampings versus $1/d$. Light and bold asterisks are the experimental data for ω_1 and ω_2 in the low-frequency Raman spectra of the NC-$Ge_{0.54}Si_{0.46}$ samples, respectively. Open circle and dashed lines are the theoretical results for the SPH mode ($l=2$, $n=1$) and filled circle and solid lines are those for the SPH mode ($l=1$, $n=2$). They are calculated using the "original" CSM model for interlayers of 1 and 0 nm, respectively. Filled and open squares show the corresponding calculated results from the modified CSM model with parameters indicated in the text.

The above experimental and theoretical results are similar to previous investigations on the interface layer between the Si NC and SiO_2 matrix which indicates that the interface layer has compositions to be between those of the crystalline Si and the SiO_2 matrix.[14,27] Thus, we tentatively introduce an interface 1–5 nm thick and the speeds of sound and density to be averages of those of the alloy NC and matrix and find that the damping does not decrease. For example, we give the data for NC-$Ge_{0.54}Si_{0.46}$ that is 7.9 nm in diameter with an interlayer that is 1 nm thick. The best candidates for ω_1 and ω_2 become the SPH modes with $n=1$, $l=2$ ($\omega'_{1\mathrm{cal}}=13.5$ cm^{-1}, $\Gamma'_{1\mathrm{cal}}=4.0$ cm^{-1}) and $n=2$, $l=1$ ($\omega'_{2\mathrm{cal}}=18.5$ cm^{-1}, $\Gamma'_{2\mathrm{cal}}=5.0$ cm^{-1}). Obviously, the reduction in damping is very limited. The experimental and theoretical results of other NC-$Ge_{0.54}Si_{0.46}$ samples with different NC central sizes are shown in Fig. 5. The disagreement is quite pronounced.

In the above calculation, we have assumed that the alloy NC is embedded in an infinite SiO_2 matrix. This assumption seems problematic because the HRTEM image in Fig. 1(g) clearly shows that the distances between neighboring NCs are only several nanometers. A coupling between the acoustic vibrations of adjacent NCs definitely exists in such a system, as the case in the 8.5 nm NC-Si/3.5 nm a-SiO_2 supperlattice.[28] Hence, the infinite SiO_2 matrix should be regarded as a composite material of SiO_2 with randomly distributed GeSi NCs embedded. This makes the impedance of the matrix larger than that of "pure" SiO_2 in the region apart from the investigated NC by a distance estimated from the NC-NC spacing. Thus, in order to consider the effect of such composite material on the damping of the NC acoustic mode we suggest a three-region model (a modified CSM model): the core is the investigated alloy NC surrounded by a pure SiO_2 shell which has a thickness to be an average distance between the neighboring NCs and the outside matrix is an effective medium representing the SiO_2 with embedded NCs. From our TEM images, the thicknesses of the middle shells for the five samples with $T_a=1100$, 1050, 1000, 950, and 900 °C are estimated to be 6.4, 4.9, 3.6, 3.2, and 2.5 nm, respectively. For the middle shell, we use the acoustic parameters of pure SiO_2, while for the matrix the parameters are weighted average ones of SiO_2 and NCs. The corresponding calculated results for the five samples are shown by full and open squares which exhibit much better consistence with the experimental data. The remarkable reduction in the damping in this modified CMS model is due to the large thickness of the middle shell reflecting the composite nature of the surrounding material.

IV. CONCLUSION

We have fabricated two groups of NC-Ge_xSi_{1-x}-embedded SiO_2 samples with different x and found that both produce two polarized size-dependent acoustic vibration modes in the low-frequency Raman spectra. Based on a large number of TEM observations, we present a three-region model in which the coupling between the acoustic vibrations of neighboring NCs is taken into account to fit the observed frequencies and dampings. Good agreement is achieved between the experiments and theory. Our experiments and theory indicate that for the nanocrystal-embedded matrix system, the low-frequency Raman spectra are closely related with both the frequencies and dampings of acoustic vibrations of NCs. This implies that low-frequency Raman scattering can be used to characterize some important parameters associated with NCs, their interfaces, and surrounding medium. Especially, it can serve as a nondestructive tool to characterize the NC sizes.

ACKNOWLEDGMENTS

The authors sincerely thank L. Saviot for providing the calculation program. This work was supported by the National and Jiangsu Natural Science Foundations (Contracts No. 60676056, No. 60576061, No. BK2008020, and No. BK2006715). Partial support was also from National Basic Research Programs of China under Grants No. 2007CB936301 and No. 2006CB921803, as well as Hong Kong RGC Competitive Earmarked Research Grant (CERG) under Contract No. CityU 112306.

*Corresponding author; hkxlwu@nju.edu.cn

[1] E. Duval, A. Boukenter, and B. Champagnon, Phys. Rev. Lett. **56**, 2052 (1986).
[2] M. Fujii, Y. Kanzawa, S. Hayashi, and K. Yamamoto, Phys. Rev. B **54**, R8373 (1996).
[3] P. Verma, W. Cordts, G. Irmer, and J. Monecke, Phys. Rev. B **60**, 5778 (1999).
[4] M. Talati and P. K. Jha, Phys. Rev. E **73**, 011901 (2006).
[5] H. Lamb, Proc. London Math. Soc. **13**, 187 (1882).
[6] X. L. Wu, Y. F. Mei, G. G. Siu, K. L. Wong, K. Moulding, M. J. Stokes, C. L. Fu, and X. M. Bao, Phys. Rev. Lett. **86**, 3000 (2001).
[7] F. Q. Liu, L. S. Liao, G. H. Wang, G. X. Cheng, and X. M. Bao, Phys. Rev. Lett. **76**, 604 (1996).
[8] Y. M. Yang, L. W. Yang, and P. K. Chu, Appl. Phys. Lett. **90**, 081909 (2007).
[9] H. K. Yadav, V. Gupta, K. Sreenivas, S. P. Singh, B. Sundarakannan, and R. S. Katiyar, Phys. Rev. Lett. **97**, 085502 (2006).
[10] Y. M. Yang, X. L. Wu, L. W. Yang, G. S. Huang, T. Qiu, Y. Shi, G. G. Siu, and P. K. Chu, J. Appl. Phys. **99**, 014301 (2006).
[11] Y. M. Yang, X. L. Wu, L. W. Yang, G. S. Huang, G. G. Siu, and P. K. Chu, J. Appl. Phys. **98**, 064303 (2005).
[12] D. B. Murray and L. Saviot, Phys. Rev. B **69**, 094305 (2004).
[13] L. Saviot, D. B. Murray, and M. C. Marco de Lucas, Phys. Rev. B **69**, 113402 (2004).
[14] N. Daldosso, M. Luppi, S. Ossicini, E. Degoli, R. Magri, G. Dalba, P. Fornasini, R. Grisenti, F. Rocca, L. Pavesi, S. Boninelli, F. Priolo, C. Spinella, and F. Iacona, Phys. Rev. B **68**, 085327 (2003).
[15] S. F. Ren, W. Cheng, and P. Y. Yu, Phys. Rev. B **69**, 235327 (2004).
[16] Y. M. Yang, X. L. Wu, L. W. Yang, and F. Kong, J. Cryst. Growth **291**, 358 (2006).
[17] Y. M. Yang, X. L. Wu, G. S. Huang, D. S. Hu, and G. G. Siu, Phys. Lett. A **338**, 379 (2005).
[18] N. N. Ovsyuk and V. N. Novikov, Phys. Rev. B **53**, 3113 (1996).
[19] R. Shuker and R. W. Gammon, Phys. Rev. Lett. **25**, 222 (1970).
[20] E. Duval, H. Portales, L. Saviot, M. Fujii, K. Sumitomo, and S. Hayashi, Phys. Rev. B **63**, 075405 (2001).
[21] N. N. Ovsyuk, E. B. Gorokhov, V. V. Grishchenko, and A. P. Shebanin, JETP Lett. **47**, 298 (1988).
[22] A. P. Sokolov, A. Kisliuk, M. Soltwisch, and D. Quitmann, Phys. Rev. Lett. **69**, 1540 (1992).
[23] We assume the elastic properties of the NC-$Ge_{0.54}Si_{0.46}$ to linearly interpolate between crystals Ge and Si. Density ρ_p and longitudinal and transverse sound speeds v_{Lp} and v_{Tp} of Ge, Si, and SiO_2 are taken to be $\bar{v}_{l,\mathrm{Ge}}=5250$ m/s, $\bar{v}_{t,\mathrm{Ge}}=3250$ m/s, $\rho_{\mathrm{Ge}}=5.33$ g/cm^3, $\bar{v}_{l,\mathrm{Si}}=9017$ m/s, $\bar{v}_{t,\mathrm{Si}}=5372$ m/s, $\rho_{\mathrm{Si}}=2.33$ g/cm^3, $\rho_{\mathrm{SiO_2}}=2.2$ g/cm^3, $\bar{v}_{l,\mathrm{SiO_2}}=5950$ m/s, and $\bar{v}_{t,\mathrm{SiO_2}}=3760$ m/s (see Ref. 22).
[24] L. Saviot and D. B. Murray, Phys. Rev. Lett. **93**, 055506 (2004).
[25] D. Vanderbilt, Phys. Rev. B **41**, 7892 (1990).
[26] J. P. Perdew, K. Burke, and M. Ernzerhof, Phys. Rev. Lett. **80**, 891 (1998).
[27] Y. Kanemitsu, H. Uto, Y. Masumoto, T. Matsumoto, T. Futagi, and H. Mimura, Phys. Rev. B **48**, 2827 (1993); Y. Kanemitsu, T. Ogawa, K. Shiraishi, and K. Takeda, *ibid.* **48**, 4883 (1993).
[28] G. F. Grom, D. J. Lockwood, J. P. McCaffrey, H. J. Labbe, P. M. Fauchet, B. White, Jr., J. Diener, D. Kovalev, F. Koch, and L. Tsybeskov, Nature (London) **407**, 358 (2000).